Basic research

Hematoporphyrin binding sites on human serum albumin

Leszek Sułkowski[1], Czesław Osuch[2], Maciej Matyja[2], Andrzej Matyja[2]

[1]Department of General Surgery, Regional Specialist Hospital, Czestochowa, Poland
[2]2nd Department of General Surgery, Jagiellonian University Medical College, Krakow, Poland

Submitted: 3 December 2019
Accepted: 2 January 2020

Arch Med Sci Civil Dis 2020; 5: e1-e7
DOI: https://doi.org/10.5114/amscd.2020.92722

Corresponding author:
Leszek Sułkowski MD, PhD
Department
of General Surgery
Regional Specialist Hospital
104/118 Bialska St
42-218 Czestochowa, Poland
Phone: +48 792244177
E-mail: leszeksulkowski@icloud.com

Abstract

Introduction: Photodynamic therapy is a minimally invasive clinical treatment modality for a variety of premalignant and malignant conditions combining a photosensitizing drug, oxygen and light irradiation. Hematoporphyrin is an organic photosensitizer, which mediates inhibition of endothelial cell proliferation and induces apoptosis. Human serum albumin is an endogenous drug carrier for hematoporphyrin. The present study aimed to investigate the hematoporphyrin binding to human serum albumin, which is its transport protein.
Material and methods: The chemical reagents were hematoporphyrin (Hp), human serum albumin (HSA) and bovine serum albumin (BSA). In the experiment two techniques were used: spectrofluorimetry and UV-Vis absorption spectrophotometry.
Results: The binding sites for Hp were identified in the tertiary structure of HSA by fluorescence quenching technique. The experiment with BSA delivered additional data on Hp-albumin interactions close to Trp135. The participation of tyrosyl residues apart from tryptophanyl ones was discussed. A decrease of the polarity in the binding sites, testifying to possible hydrogen bonding in the binding sites, was also described. The binding and quenching constants Hp-HSA and Hp-BSA were determined as well as the number of binding sites.
Conclusions: Hp locates in subdomain IIA in the tertiary structure of HSA. The location in subdomain I close to Trp135 is also possible. Hp is also able to interact within tyrosyl residues.

Key words: photodynamic therapy, photosensitizer, human serum albumin, bovine serum albumin, photodynamic diagnosis, hematoporphyrin, emission fluorescence.

Introduction

Photodynamic therapy (PDT) is a minimally invasive clinical treatment modality for a variety of premalignant and malignant conditions [1, 2]. It combines a photosensitizing drug, which selectively accumulates in tumor tissue and sensitizes it to light, oxygen ($^3O_2$) and laser light irradiation to produce highly reactive singlet oxygen ($^1O_2$). It leads to destruction of cellular membranes and intracellular organelles, DNA damage and finally destruction of target cells [1, 3, 4].

PDT has been approved to treat patients with variety of early stages of precancerous lesions and cancers of lungs, esophagus (including Barrett's esophagus), rectum and colon, breast, skin, head and neck, urinary

bladder, female reproductive tract and pancreas [1–9]. PDT may also be applied in the palliative care of cancers in the above-mentioned locations. Another indication for PDT is the treatment of microbiological infections of burns, wounds and ulcers [3, 10].

Clinical outcomes of PDT may remain suboptimal, either insufficient or excessive, and depend on local photosensitizer concentration in the target tissue, local tissue oxygenation and local light fluence [1]. PDT has good tolerance and mild adverse effects, minimizes the risk of complications, improves quality of life and should be considered as an effective alternative treatment [2, 3, 5, 6]. However, PDT is still not considered in some guidelines due to the large variety of PDT parameters, including photosensitizer concentration and dosage of light [3]. Knowledge of the mechanisms of absorption and distribution of photosensitizers allows maximal efficiency of the photodynamic response to be achieved [11].

Porphyrins, which include hematoporphyrin (Hp), are the best-studied group of photosensitizers. Hp is an organic photosensitizer, which mediates inhibition of endothelial cell proliferation in PDT and induces apoptosis [2, 4, 12–14]. Hp has good efficacy and a low recurrence rate [14]. In accordance with the general rule of systemic injection of a photosensitizer in PDT, Hp is administered intravenously [6, 15].

Serum albumins (SA) constitute 55–65% of all serum proteins. Their physiological concentration of 40–50 g/l is a result of food supply, absorption, distribution between plasma and interstitial fluid as well as degradation. The human serum albumin (HSA) molecule with a molecular mass of 67000 Da consists of 585 amino acid residues forming one polypeptide chain, of which 67% form the α helical structure. The HSA polypeptide chain is formed in the shape of a 80 × 80 × 80 × 30 Å heart [16–18]. The albumin molecule contains three structurally homologous domains: I, II and III. Each of these domains is formed by two subdomains: A and B. Subdomains A and B consist of 4 and 6 α helices, respectively [16–18]. Each subdomain A is wider than subdomain B [19]. SAs of other species (e.g. bovine, horse, mouse, dog, salmon, frog) have a repeating amino acid sequence [20]. Bovine serum albumin (BSA) has the most similar structure to HSA. The structure of HSA and BSA is 76% identical. The molecular weight of BSA is 66500 Da. The BSA amino acid sequence contains two tryptophans (Trps), Trp135 and Trp214, while HSA contains Trp214 only [21].

One of the most important properties of albumin is the ability to bind and transport many endo- and exogenous compounds lacking specific transport proteins. Endogenous compounds include fatty acids, bilirubin, uric acid, hormones, vitamins, and metal ions (Ca^{2+}, Cu^{2+}, Zn^{2+}). Exogenous ligands are primarily drugs (e.g. salicylates, sulfonamides, antibiotics) and contrast agents, including photosensitizers [22–25]. The complex formed between ligand and albumin protects the ligand against oxidation, reduces its toxicity, increases its solubility in the serum and therefore improves its transport [26].

The present spectroscopic study aimed to investigate the binding of Hp to HSA, which is its transport protein, determine the loci of Hp binding in the tertiary structure of the albumin and study the interactions in Hp-HSA complexes.

Material and methods

Chemical reagents

Hematoporphyrin, molecular weight 598.71 Da, was purchased from Sigma-Aldrich Inc. St. Louis, USA. Human serum albumin, fraction V, molecular weight 67000 Da, was obtained from ICN Biomedical Inc. Aurora, USA. Bovine serum albumin, molecular weight 66500 Da, was obtained from Biomed Lublin, Poland.

Absorption spectra

The absorption UV-Vis spectra were recorded with Jasco V-530 spectrometer (Jasco International Co., Ltd., Tokyo, Japan). The UV-Vis spectra of HSA, BSA and Hp were recorded in the wavelength range 210-690 nm, 30 min after sample preparation, at 25°C. Correcting error of apparatus for the wavelength (λ) is ±1 nm, while for the absorbance (A) it is ±0.00001.

Fluorescence analysis

The emission fluorescence spectra were recorded with Kontron SFM-25 Instrument AG (Kontron AG, Zurich, Switzerland) 30 min after preparation of the solutions, at 25°C. Correcting error of apparatus for the wavelength (λ) is ±1 nm, while for the relative fluorescence (RF) it is ±0.01.

To excite fluorophores two wavelengths were used: λ_{ex} = 280 nm and 295 nm. The emission spectra were recorded in the wavelength range 280–400 nm and 295–400 nm for λ_{ex} = 280 nm and 295 nm, respectively. The concentration was adjusted to produce an absorbance ($A \leq 0.05$) and the fluorescence spectra were not corrected for the inner filter effect [27].

The best solubility of Hp was obtained in phosphate buffer 0.05 M, pH 7.40. This buffer was used to prepare solutions of Hp and both SAs.

In the study of Hp binding to HAS and BSA the concentration range of Hp was 0 to 9×10^{-5} M and 0 to 5×10^{-5} M, respectively.

For each BSA solution from 5 × 10^{-7} M to 1 × 10^{-7} M the samples containing Hp within the concentration range from 0 to 5 × 10^{-5} M were prepared. For each HSA solution from 2.5 × 10^{-6} M to 2.5 × 10^{-7} M the samples containing Hp within the concentration range from 0 to 9 × 10^{-5} M were prepared.

The association constant (K_a) was determined by the Scatchard method modified by Hiratsuka [28]:

$$\frac{r}{L_f} = nK_a - K_a r \quad \text{(eq. 1)}$$

where: r – fractional saturation of sites; $r = \Delta RF/\Delta RF_{max}$ (where: $\Delta RF = RF - RF_0$; $\Delta RF_{max} = RF_{max} - RF_0$); $[L_f]$ – free ligand concentration; K_a – association constant; n – number of binding sites for the independent class of ligand binding sites in the albumin molecule, which corresponds to the mean number of ligand molecules bound to the independent class of ligand binding sites in the albumin molecule.

The fluorescence quenching effect and the Stern-Volmer constants were estimated based on the Stern-Volmer equation (eq. 2), which allows one to describe ligand movement within the fluorophore microenvironment upon dynamic quenching [29]:

$$\frac{RF_0}{RF} = 1 + k_q\tau_0[Q] = 1 + K_Q[Q] \quad \text{(eq. 2)}$$

where: RF_0 and RF – fluorescence intensities in the absence and presence of the quencher (Q), respectively; k_q – rate quenching constant (M^{-1} s^{-1}); τ_0 – fluorescence lifetime in the absence of quencher; K_Q – quenching constant; [Q] – quencher (Hp) concentration.

The Stern-Volmer equation modified by Lehrer [30] was used to determine the quenching constant (K_Q):

$$\frac{RF_0}{\Delta RF} = \frac{1}{[Q]} \cdot \frac{1}{\int_a} \cdot \frac{1}{K_Q} + \frac{1}{\int_a} \quad \text{(eq. 3)}$$

where: RF_0 and RF – fluorescence intensities in the absence and presence of the quencher (Q), respectively; ΔRF – difference between RF_0 and RF; $\int_a$ – fractional accessible protein fluorescence; K_Q – quenching constant; [Q] – quencher (Hp) concentration.

Results and discussion

Quenching fluorescence study – complex formation

Spectrofluorimetry was used to study the complex formation between Hp and both BSA and HSA. The emission fluorescence spectra of HSA

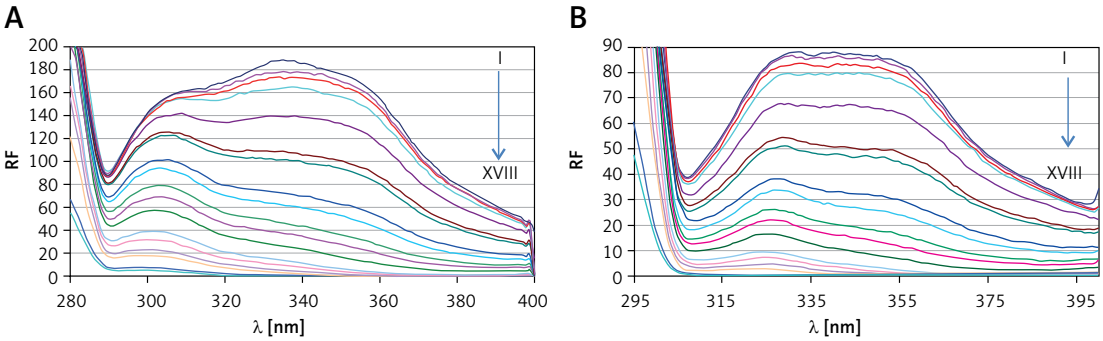

Figure 1. Quenching of HSA fluorescence (at concentration 1.25 × 10^{-6} M) excited at λ_{ex} = 280 nm (**A**) and λ_{ex} = 295 nm (**B**) in the presence of Hp within concentration range from 0 to 9 × 10^{-5} M (I – 0 M; II – 2 × 10^{-8} M; III – 5 × 10^{-8} M; IV – 1 × 10^{-7} M; V – 5 × 10^{-7} M; VI – 1 × 10^{-6} M; VII – 1.5 × 10^{-6} M; VIII – 3.5 × 10^{-6} M; IX – 5 × 10^{-6} M; X – 7.5 × 10^{-6} M; XI – 1 × 10^{-5} M; XII – 1.5 × 10^{-5} M; XIII – 2.5 × 10^{-5} M; XIV – 3 × 10^{-5} M; XV – 4 × 10^{-5} M; XVI – 5 × 10^{-5} M; XVII – 8 × 10^{-5} M; XVIII – 9 × 10^{-5} M)

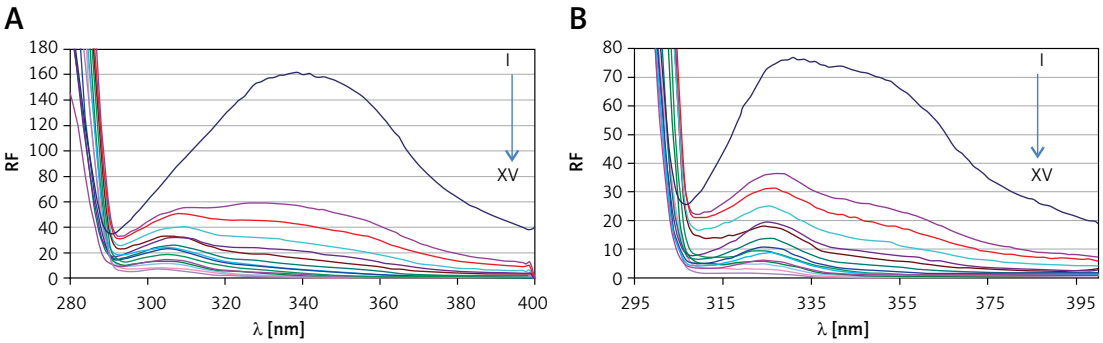

Figure 2. Quenching of BSA fluorescence (at concentration 4 × 10^{-7} M) excited at λ_{ex} = 280 nm (**A**) and λ_{ex} = 295 nm (**B**) in the presence of Hp within concentration range from 0 to 5 × 10^{-5} M (I – 0 M; II – 1 × 10^{-6} M; III – 1.5 × 10^{-6} M; IV – 2.5 × 10^{-6} M; V – 3.5 × 10^{-6} M; VI – 5 × 10^{-6} M; VII – 7.5 × 10^{-6} M; VIII – 1 × 10^{-5} M; IX – 1.25 × 10^{-5} M; X – 1.5 × 10^{-5} M; XI – 2 × 10^{-5} M; XII – 2.5 × 10^{-5} M; XIII – 3 × 10^{-5} M; XIV – 4 × 10^{-5} M; XV – 5 × 10^{-5} M)

excited at λ_{ex} = 280 nm and 295 nm have signals at λ_{max} = 334–336 nm and λ_{max} = 343–345 nm, respectively (Figures 1 A, B). The emission fluorescence spectra of BSA excited at λ_{ex} = 280 nm and 295 nm have signals at λ_{max} = 333–339 nm and λ_{max} = 326–333 nm, respectively (Figures 2 A, B).

For the above presented solutions of SAs and Hp the fluorescence quenching curves, Stern-Volmer curves and Scatchard curves have been plotted and discussed below.

Two binding sites for ligands were initially described by Sudlow: the first was a "warfarin binding site", while the second was the "benzodiazepine binding site" [31]. Site I is a hydrophobic niche containing Trp214 (in both HSA and BSA molecules) and is located in subdomain IIA [32]. Site I is very flexible and presents high adaptability to the ligand [33]. Site II can bind smaller organic molecules. The flexibility of site II is much lower [34].

The changes in HSA emission fluorescence upon binding Hp are shown in Figures 1 A and B for λ_{ex} = 280 nm and 295 nm, respectively. A similar effect is observed for BSA (Figures 2 A and B for λ_{ex} = 280 nm and 295 nm, respectively).

The HSA fluorescence has been compared to its fluorescence quenched by Hp (Figures 1 A, B). Fluorescence of HSA excited at λ_{ex} = 280 nm is quenched by Hp to 10.9%, 4.7% and 3.3% of its initial value at the Hp : HSA molar ratios 40 : 1, 64 : 1 and 72 : 1, respectively (Figures 1 A, 3 A, 4 A). Fluorescence of HSA excited at λ_{ex} = 295 nm decreases to 10.8%, 8.4%, 5.2% and 3.3% of the initial value at Hp : HSA molar ratios 20 : 1, 24 : 1, 32 : 1 and 40 : 1 for HSA concentration 4 × 10^{-7} M (Figures 1 B, 3 B, 4 A).

For molar ratios of Hp : BSA 62.5 : 1, 75 : 1, 100 : 1 and 125 : 1 BSA fluorescence excited at λ_{ex} = 280 nm reaches respectively 8.5%, 7.3%, 5.5% and 4.4% of the initial value for BSA concentration 4 × 10^{-7} M (Figures 2 A, 3 A, 4 B). Fluorescence of BSA excited at λ_{ex} = 295 nm is quenched to 7.5%, 6.2%, 4.2% and 2.3% of the initial value for Hp : BSA molar ratios 62.5 : 1, 75 : 1, 100 : 1 and 125 : 1 (Figures 2 B, 3 B, 4 B).

The quenching of the fluorescence of both albumins is positively correlated with Hp concentration in the Hp-HSA and Hp-BSA solutions (Figures 1 and 2, respectively) and may be explained by the energy transfer from HSA and BSA fluorophores to Hp chromophores [35]. This energy transfer may appear when the distance between fluorophores in the macromolecule of albumins and micromolecule of Hp does not exceed 10 nm, which is almost equal to the distance of van der Waals forces [36]. The experiment showed that fluorophores of Hp receive energy from excited HSA and BSA fluorophores. This phenomenon has been discussed by Eftink [36, 37] in the experiment of energy transfer from indole excited at λ_{ex} = 295 nm to acrylamide. In Eftink's experiment the indole acts as a model of an albumin, because

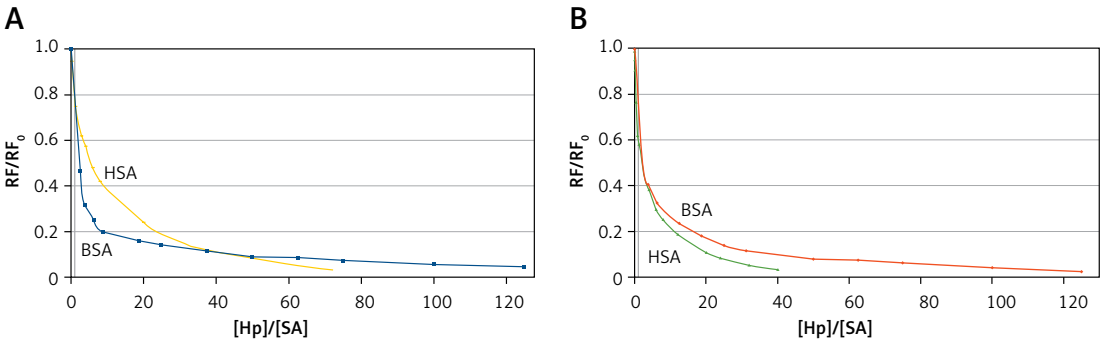

Figure 3. HSA and BSA fluorescence quenching curves by Hp, λ_{ex} = 280 nm (**A**) and λ_{ex} = 295 nm (**B**)

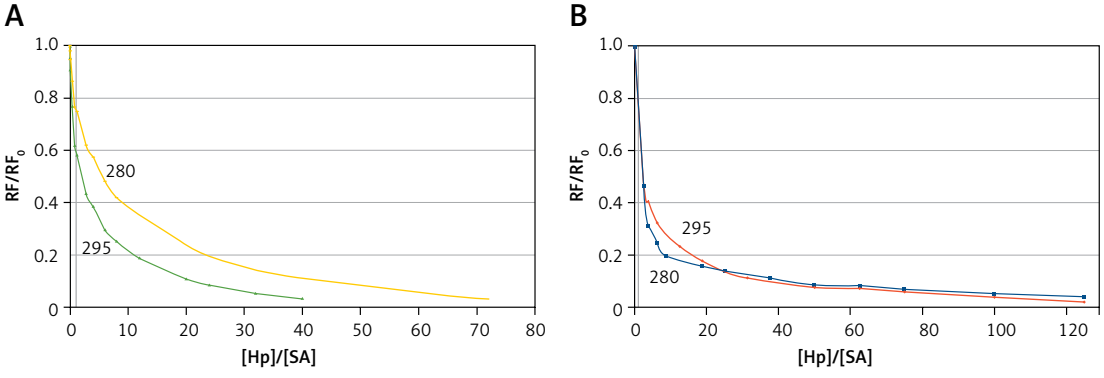

Figure 4. HSA (**A**) and BSA (**B**) fluorescence quenching curves by Hp for λ_{ex} = 280 nm and λ_{ex} = 295 nm

the tryptophanyl residues in the primary structure of albumin contain indole rings.

To indicate the binding site of the Hp in the tertiary structure of the HSA the difference in the primary structure of both albumins (i.e. HSA and BSA) was taken into account. HSA contains one tryptophanyl group (Trp214) located in subdomain IIA, while BSA contains a second one (Trp135) in subdomain IB [19, 38]. Comparison of changes in fluorescence quenching of both albumins differing in the number of tryptophanyl groups allowed us to indicate the binding site of Hp in their structure.

Hp quenches fluorescence of HSA excited at λ_{ex} = 280 nm less than BSA up to molar ratio Hp : SA 40 : 1 (Figure 3 A). For a higher molar ratio HSA fluorescence is quenched more than that of BSA (Figure 3 A). An explanation of this difference may be the presence of two tryptophanyl groups (Trp135 and Trp214) in BSA and only one (Trp214) in HSA, apart from tyrosine (Tyr) groups excited at λ_{ex} = 280 nm. Greater quenching of fluorescence of BSA containing two tryptophanyl groups (Trp135 and Trp214) indicates that the Hp molecules localize close to both Trps present in the BSA tertiary structure in subdomains IB and IIA. It can therefore be assumed that Hp has probably two binding sites in the tertiary structure of BSA and HSA, located in subdomains IB and IIA. In HSA fluorescence quenching is weaker, because HSA contains only Trp214 located in subdomain IIA. This means that spectroscopic information for HSA can only be obtained from subdomain IIA. For λ_{ex} = 295 nm, HSA fluorescence is quenched more than that of BSA (Figure 3 B).

Interactions of Hp at the binding sites in the structure of HSA and BSA

A comparison between quenching of SA fluorescence excited at λ_{ex} = 280 nm and 295 nm, causing excitation of both Tyrs and Trps and only Trps, respectively, gave information on the participation of tyrosyl and tryptophanyl residues in the interactions in complexes of both albumins with Hp.

Comparing the quenching of the BSA fluorescence excited at two wavelengths λ_{ex} = 280 nm and λ_{ex} = 295 nm by Hp (Figure 4 B), three ranges of Hp:BSA molar ratios were found. The overlapping quenching curves BSA-Hp might point to a lack of interaction between Hp and tyrosyl residues in BSA for a molar ratio below 5 : 1 and over 25 : 1 (Figure 4 B). Higher quenching of BSA fluorescence excited at λ_{ex} = 280 nm than that at λ_{ex} = 295 nm in the molar range Hp : BSA 5 : 1–25 : 1 points to the participation of tyrosyl groups in the interaction between Hp and BSA.

The HSA fluorescence excited at λ_{ex} = 295 nm decreases in the presence of Hp more than that at λ_{ex} = 280 nm (Figure 4 A). Nearly complete (96.7%) quenching of HSA fluorescence at λ_{ex} = 280 nm by Hp occurs at a molar ratio Hp : HSA 72 : 1, while at λ_{ex} = 295 nm a similar effect was observed at a molar ratio Hp : HSA 40 : 1. This suggests that the tertiary structure of BSA is altered in the presence of Hp and the binding subdomain changes its geometry when the complex with Hp forms. The change in the geometry of the binding site can be caused by the dimerization of Hp at concentrations exceeding 4×10^{-5} M, which was previously described by Silla *et al.* [39].

The decrease of HSA and BSA fluorescence by Hp at concentration 8×10^{-5} M is accompanied by a blue shift of the maximum fluorescence emission by 9 nm and 11 nm, respectively (Figures 1 B, 2 B). Since the effect is observed at λ_{ex} = 295 nm the conclusions concern subdomains IB and IIA where Trp 135 and Trp214 are located. The bathochromic shift of the maximum of albumin fluorescence has been observed for albumin solutions in polar solvents [40]. Chadborn *et al.* explained the hypsochromic shift of the maximum fluorescence of Trp caused by different ligands by the increase in the hydrophobicity of the Trp environment [41]. The shift of the maximum of albumin fluorescence caused by Hp allowed assessment of the changes in the hydrophobic environment of the fluorophores of albumins. Hp can form hydrogen bonding not only with polar residues in the binding subdomain, but also with peptide bonds in SA.

Table I. Association constants (K_a), number of binding sites (n) and quenching constants (K_Q) in the Hp complexes with HSA and BSA

HSA-Hp		BSA-Hp	
λ_{ex} = 280 nm	λ_{ex} = 295 nm	λ_{ex} = 280 nm	λ_{ex} = 295 nm
$K_{a\,I} = 9.31 \times 10^5$ M^{-1} $n_I = 0.54$ $K_{a\,II} = 1.35 \times 10^5$ M^{-1} $n_{II} = 1.0$	$K_{a\,I} = 5.37 \times 10^6$ M^{-1} $n_I = 0.61$ $K_{a\,II} = 4.90 \times 10^5$ M^{-1} $n_{II} = 1.1$	$K_{a\,I} = 3.77 \times 10^6$ M^{-1} $n_I = 0.87$ $K_{a\,II} = 8.18 \times 10^5$ M^{-1} $n_{II} = 1.1$	$K_{a\,I} = 2.43 \times 10^6$ M^{-1} $n_I = 0.81$ $K_{a\,II} = 6.94 \times 10^5$ M^{-1} $n_{II} = 1.1$
$K_Q = 2.52 \times 10^6$ M^{-1}	$K_Q = 2.08 \times 10^5$ M^{-1}	$K_Q = 2.01 \times 10^6$ M^{-1}	$K_Q = 6.35 \times 10^5$ M^{-1}

Association constants (K_a) and quenching constants (K_Q)

Eftink and Ghiron formulated a hypothesis that the increase in the number of sites occupied in the molecule decreases quenching of fluorescence [36, 37]. To verify this hypothesis the Stern-Volmer equations was analyzed. The quenching constant (K_Q) was determined by the Stern-Volmer method modified by Lehrer (eq. 3) [30].

The Scatchard curve analysis gave information on the number of classes of binding sites for both Hp-BSA and Hp-HSA complexes. The strength of binding between the ligand and albumin was calculated using the Scatchard method (eq. 1) [28]. The number of moles of ligands bound to one mole of albumin in the analyzed binding site was determined based on the Scatchard curves analysis.

To assess the stability and binding strength of Hp with HSA and BSA, the association constants (K_a) and quenching constants (K_Q) for both complexes Hp-HSA and Hp-BSA were determined by analyzing the Scatchard (eq. 1) and Stern-Volmer equations (eq. 3) (Table I). The K_a values are relatively high. They are of the order 10^5 and 10^6 (M^{-1}). This may point to rather strong interaction between Hp and serum albumins. This confirms the suggestion that Hp may interact with the peptide bond in albumin by hydrogen bonding.

The Scatchard curve analysis shows two classes of binding sites for both HSA and BSA (Table I). The K_a for Hp binding with HSA and BSA was determined for λ_{ex} = 280 nm and 295 nm for both classes of binding sites (Table I).

There was lower for HSA (n_I = 0.54–0.61) and higher for BSA (n_I = 0.81–0.87) affinity of Hp in the first class of binding sites and the same (n_{II} = 1.0–1.1) affinity in the second class (Table I). The higher number of Hp molecules in I class binding sites in BSA compared to HSA may be explained by the experiment that allowed us to observe different subdomains in BSA and HSA where Trps and Tyrs residues are located (i.e. IB, IIA and IIIA). The values of K_a indicate that between Hp and both albumins the complexes are formed. Probably the ϖ-ϖ interactions are supported by hydrogen bonds, as indicated by the existence of two classes of binding sites.

The comparison of K_a values for BSA and HSA shows that the binding of Hp to BSA is respectively 3.1-fold higher than for HSA in the first class of binding sites for λ_{ex} = 280 nm and 2.2-fold lower than HSA in the first class of binding sites for λ_{ex} = 295 nm. In the second class of binding sites binding of Hp to BSA is 6- and 1.4-fold higher than to HSA for λ_{ex} = 280 nm and 295 nm, respectively. Larger K_Q values (for both HSA and BSA) were obtained for λ_{ex} = 280 nm than for λ_{ex} = 295 nm. The difference may be a result of higher accessibility to fluorophores in the protein excited at 280 nm than 295 nm.

In conclusion, the quenching of SA fluorescence by Hp points to the conclusion that Hp interacts with HSA in its subdomain IIA where Trp214 is located. The location in subdomain IA close to Trp135 is also possible. Hp is also able to interact within tyrosyl residues as demonstrated by the comparison of the quenching of SA fluorescence excited at 280 nm and 295 nm.

Two classes of binding sites for Hp with different affinity towards HSA were identified. The Hp-HSA complex is stabilized by both hydrophobic interactions and hydrogen bonds between Hp and HSA. The BSA study enabled observation of interactions with Hp within subdomain IB of the albumin.

A decrease of the polarity around the fluorophores in the binding site results from the possible hydrogen bonding between Hp and peptide bonds in SA. This is confirmed by the values of binding constants K_a being of the order 10^5 and 10^6 (M^{-1}).

The obtained data on formation of the Hp-HSA complex, location of the Hp molecule in the tertiary structure of the HSA molecule, and the nature of interactions between Hp and HSA are crucial for understanding transportation of Hp to the cancer tissue. However, future clinical trials are needed.

Conflict of interest

The authors declare no conflict of interest.

References

1. Ong YH, Kim MM, Finlay JC, et al. PDT dose dosimetry for Photofrin-mediated pleural photodynamic therapy (pPDT). Phys Med Biol 2017; 63: 015031.
2. Hosokawa S, Takebayashi S, Takahashi G, Okamura J, Mineta H. Photodynamic therapy in patients with head and neck squamous cell carcinoma. Lasers Surg Med 2018; 50: 420-6.
3. Ye X, Yin H, Lu Y, Zhang H, Wang H. Evaluation of hydrogel suppositories for delivery of 5-aminolevulinic acid and hematoporphyrin monomethyl ether to rectal tumors. Molecules 2016; 21: pii:1347.
4. Lin C, Zhang Y, Zhu X, et al. The study of killing effect and inducing apoptosis of 630-nm laser on lung adenocarcinoma A549 cells mediated by hematoporphyrin derivatives in vitro. Lasers Med Sci 2019 May 2.
5. Gross SA, Wolfsen HC. The use of photodynamic therapy for diseases of the esophagus. J Environ Pathol Toxicol Oncol 2008; 27: 5-21.
6. Liu H, Liu Y, Wang L, et al. Evaluation on short-term therapeutic effect of 2 porphyrin photosensitizer-mediated photodynamic therapy for esophageal cancer. Technol Cancer Res Treat 2019; 18: 1533033819831989.
7. Railkar R, Agarwal PK. Photodynamic therapy in the treatment of bladder cancer: past challenges and current innovations. Eur Urol Focus 2018; 4: 509-11.

8. DeWitt JM, Sandrasegaran K, O'Neil B, et al. Phase 1 study of EUS-guided photodynamic therapy for locally advanced pancreatic cancer. Gastrointest Endosc 2019; 89: 390-8.
9. Yang J, Shen H, Jin H, Lou Q, Zhang X. Treatment of unresectable extrahepatic cholangiocarcinoma using hematoporphyrin photodynamic therapy: a prospective study. Photodiagnosis Photodyn Ther 2016; 16: 110-8.
10. Ma W, Wang T, Zang L, et al. Bactericidal effects of hematoporphyrin monomethyl ether-mediated blue-light photodynamic therapy against Staphylococcus aureus. Photochem Photobiol Sci 2019; 18: 92-7.
11. Sułkowski L, Pawełczak B, Chudzik M, Maciążek-Jurczyk M. Characteristics of the protoporphyrin IX binding sites on human serum albumin using molecular docking. Molecules 2016; 21: pii:E1519.
12. Ma G, Han Y, Ying H, et al. Comparison of two generation photosensitizers of psd-007 and hematoporphyrin monomethyl ether photodynamic therapy for treatment of port-wine stain: a retrospective study. Photobiomodul Photomed Laser Surg 2019; 37: 376-80.
13. Mei Y, Xiao X, Fan L, et al. In vitro photodynamic therapy of endothelial cells using hematoporphyrin monomethyl ether (Hemoporfin): relevance to treatment of port wine stains. Photodiagnosis Photodyn Ther 2019; 27: 268-75.
14. Ma J, Lai G, Lu Z. Effect of 410 nm photodynamic therapy with hemoporfin on the expression of vascular endothelial growth factor (VEGF) in cultured human vascular endothelial cells. Lasers Med Sci 2019; 34: 149-55.
15. Kim D, Lee MH, Koo MA, et al. Suppression of T24 human bladder cancer cells by ROS from locally delivered hematoporphyrin-containing polyurethane films. Photochem Photobiol Sci 2018; 17: 763-72.
16. He XM, Carter DC. Atomic structure and chemistry of human serum albumin. Nature 1992; 358: 209-14.
17. Geisow MJ. Human serum albumin structure. Trends Biotechnol 1992; 10: 335-7.
18. Carter DC, Ho JX. Structure of serum albumin. Adv Protein Chem 1994; 45: 153-203.
19. de Wolf FA, Brett GM. Ligand-binding proteins. Their potential for application in systems for controlled delivery and uptake of ligands. Pharmacol Rev 2000; 52: 207-36.
20. Równicka-Zubik J, Sułkowski L, Maciążek-Jurczyk M, Sułkowska A. The effect of structural alterations of three mammalian serum albumins on their binding properties. J Mol Structure 2013; 1044: 152-9.
21. Równicka-Zubik J, Sułkowska A, Maciążek-Jurczyk M, Sułkowski L, Sułkowski WW. Effect of denaturating agents on the structural alterations and drug binding capacity of human and bovine serum albumin. Int J Rapid Commun 2012; 45:520-9.
22. Marciniec K, Pawełczak B, Latocha M, et al. Quinolinesulfonamides: interaction between bovine serum albumin, molecular docking analysis and antiproliferative activity against human breast carcinoma cells. Spectroscopy Letters 2017; 50(10).
23. Równicka-Zubik J, Sułkowski L, Toborek M. Interactions of PCBs with human serum albumin: in vitro spectroscopic study. Spectrochim Acta A Mol Biomol Spectroscopy 2014; 124: 632-7.
24. Sułkowski L, Sułkowska A, Rownicka J, et al. The effect of serum albumin on binding of protoporphyrin IX to phospholipid membrane. Mol Cryst Liq Cryst 2006; 448: 73[675]-81[683].
25. Sułkowska A, Drzazga Z, Maciążek M, Równicka J, Bojko B, Sułkowski L. Porphyrin IX – serum albumin interactions. Phys Med 2004; 20 Suppl. 1: 49-51.
26. Sułkowski L, Równicka-Zubik J, Pawełczak B, Pożycka J, Sułkowska A. Effect of encapsulation on phase transition temperature of liposomes. Binding sites in HSA. Mol Cryst Liq Cryst 2014; 603: 105-21.
27. Steinem RF, Weinryb I, Kirby EP (eds). Fluorescence Instrumentation and Methodology, Inc. Maryland, 1970; 39-42.
28. Hiratsuka T. Conformational changes in the 23-kilodalton NH2-terminal peptide segment of myosin ATP-ase associated with ATP hydrolysis. J Biol Chem 1990; 265: 18786-90.
29. Eftink MR, Ghiron CA. Exposure of tryptophanyl residues in proteins. Quantitative determination by fluorescence quenching studies. Biochemistry 1976; 15: 672-80.
30. Lehrer SS. Solute perturbation of protein fluorescence. The quenching of the tryptophyl fluorescence of model compounds and of lysozyme by iodide ion. Biochemistry 1971; 10: 3254-63.
31. Sudlow G, Birkett DG, Wade DN. The characterization of two specific drug binding sites on human serum albumin. Mol Pharmacol 1975; 11: 824-32.
32. Sugio S, Kashima A, Mochizuki S, Noda M, Kobayashi K. Crystal structure of human serum albumin at 2.5 Ã resolution. Protein Eng 1999; 12: 439-46.
33. Kragh-Hansen U. Evidence for a large and flexible region of human serum albumin possessing high affinity binding sites for salicylate, warfarin, and other ligands. Mol Pharmacol 1988; 34: 160-71.
34. Kragh-Hansen U, Chuang VT, Otagiri M. Practical aspects of the ligand-binding and enzymatic properties of human serum albumin. Biol Pharm Bull 2002; 25: 695-704.
35. Valeur B. Molecular fluorescence. Principles and applications. Weinheim, Wiley-VCH 2002.
36. Eftink MR, Ghiron CA. Exposure of tryptophanyl residues in proteins. Quantitative determination by fluorescence quenching studies. Biochemistry 1976; 15: 672-80.
37. Eftink MR, Ghiron CA. Fluorescence quenching studies with proteins. Anal Biochem 1981; 114: 199-227.
38. Carter DC, He XM. Structure of serum albumin. Science 1990; 249: 302-3.
39. Sil S, Kar M, Chakraborti AS. Studies on the interaction of hematoporphyrin with hemoglobin. J Photochem Photobiol B 1997; 41: 67-72.
40. Guharay J, Sengupta PK. Characterization of the fluorescence emission properties of 7-azatryptophan in reverse micellar environments. Biochem Biophys Res Commun 1996; 219: 388-92.
41. Chadborn N, Bryant J, Bain AJ, O'Shea P. Ligand-dependent conformational equilibria of serum albumin revealed by tryptophan fluorescence quenching. Biophys J 1999; 76: 2198-207.